Report MPIK - V30 - 1995

The Cosmic Ray Tracking detector system

K. Bernlöhr, S. Gamp, G. Hermann, W. Hofmann, T. Kihm,
J. Knöppler, G. Leffers, V. Matheis, M. Panter,
U. Trunk, M. Ulrich, T. Wolf, R. Zink
Max-Planck-Institut für Kernphysik, Heidelberg, Germany

J. Heintze, P. Lennert, S. Polenz
*Physikalisches Institut, Universität Heidelberg,
Heidelberg, Germany*

R. Eckmann
*II. Institut für Experimentalphysik, Universität Hamburg,
Hamburg, Germany*

July 12, 1995

Abstract

The Cosmic Ray Tracking (CRT) project represents a study on the use of tracking detectors of the time projection chamber type to detect secondary cosmic ray particles in extensive air showers. In reconstructing the arrival direction of the primary cosmic ray particles, the CRT detectors take advantage of the angular correlation of secondary particles with the cosmic rays leading to these air showers.

In this paper, the detector hardware including the custom-designed electronics system is described in detail. A CRT detector module provides an active area of $2.5\,\mathrm{m}^2$ and allows to measure track directions with a precision of $0.4°$. It consists of two circular drift chambers of $1.8\,\mathrm{m}$ diameter with six sense wires each, and a $10\,\mathrm{cm}$ thick iron plate between the two chambers. Each detector has a local electronics box with a readout, trigger, and monitoring system.

The detectors can distinguish penetrating muons from other types of charged secondaries. A large detector array could be used to search for γ-ray point sources at energies above several TeV and for studies of the cosmic-ray composition. Ten detectors are in operation at the site of the HEGRA air shower array. The online software and the detector performance are described in a subsequent paper.

1 Introduction

After observations of point-like sources of high-energy (up to $1\,\mathrm{GeV}$) γ-rays by the SAS-2 and COS-B satellites an increasing number of astronomers and physicists became interested in cosmic ray research. Due to the rapidly falling energy spectrum of cosmic rays the field remains divided into small-area satellite and balloon experiments for the MeV and GeV region and large-area ground and underground experiments for the TeV and PeV regimes.

The first kind of experiments can easily distinguish between the γ, $e^{\pm}$, and nuclear components of the cosmic radiation. However, they run out of statistics at high energies (near 10 GeV for γ-rays sources and near 10–100 TeV for the isotropic charged cosmic rays) due to their small detector areas.

At very high energies (above a few 10^{11} eV) the atmosphere is used as the target medium for cosmic ray particles and secondary products of the *Extensive Air Showers* (EAS) are observed on ground (secondary particles in the shower as well as Cherenkov and fluorescence light) and under ground or under water (muons and neutrinos). These experiments have sensitive areas many orders of magnitudes larger than satellite experiments but to distinguish between different kinds of primary particles is very difficult. Therefore, little is known about the cosmic ray composition above about 100 TeV (10^{14} eV) [1]. Due to the isotropic background of charged cosmic rays, the search for γ-ray point sources is also difficult with these experiments [2].

After initial claims of ground-based detections of point sources which remained unconfirmed or ambiguous, it became obvious that a substantial effort was necessary to achieve clear detections of sources. The main advances in recent years, as far as ground-based experiments are concerned, are the use of photomultiplier cameras in imaging *Atmospheric Cherenkov Telescopes* (ACT), the build-up of larger scintillator arrays – some with additional large-area muon counters – and the development of new detection techniques, such as wide-angle non-imaging atmospheric Cherenkov counters, water Cherenkov detectors, drift chambers, and resistive-plate chambers, to name just a few. Due to the still existing gap between the energy ranges of ACTs (about 0.3–5 TeV) and of scintillator arrays (above about 30 TeV) many of these new techniques were developed to access the energy range around 10^{13} eV.

Only by the ACT technique – with image analysis to reduce the strong hadronic background of charged cosmic rays – a few unambiguous sources of γ-rays in the TeV energy range have been detected. No clear sources have been found by the scintillator arrays which have much larger thresholds, usually between 30 TeV and about 200 TeV.

For several important astrophysical questions like the cutoff of source spectra and the transparency of the intergalactic medium for very-high-energy γ-rays, efficient detection techniques in the energy range between a few TeV and some 100 TeV are needed. One of the detector concepts for this purpose is that of an array of tracking detectors, the CRT array, proposed in 1988 [3, 4, 5].

Since the proposal of CRT, several prototype detectors have been built and tested. Two detector variants, identical in the basic drift chamber but with different detector vessels and readout systems, have been studied by the Max Planck Institute (MPI) and the University of Heidelberg groups, respectively. This paper deals only with the MPI variant of the detector. However, differences in the basic performance are small. Detectors and readout system of the University variant are described in detail in [6]. A complete chain of electronics for detector readout and operation has been developed at the Max Planck Institute and a first series of 10 detectors has been brought into operation. In this first phase of CRT, the TPC technique [7], which was previously only used in the strictly controlled environment of very expensive particle accelerator experiments, has been developed into an inexpensive, robust detector which can be built in large numbers.

After a short summary of the CRT concepts, this paper describes in detail the detector modules and the electronics and readout system developed for CRT. The online software for readout, track reconstruction, and detector calibration are presented in another paper [8] (in the following referred to as Paper II), as well as Monte-Carlo detector simulations. The detector performance derived from measurements with the 10 detectors operated at the HEGRA experiment [9] on La Palma, Canary Islands, is also described in Paper II.

2 The CRT detector and array concepts

The basic concept of the CRT project is that by the tracking method, i.e. by observing the arrival directions of secondary particles, air showers can be reconstructed with much fewer observed secondaries than needed for scintillator arrays. Secondary particles in air showers propagate approximately along the direction of the primary particle. While for existing scintillator arrays some 10^4 charged particles arriving at ground level are needed, only some 10^3 are required for a CRT array of several hundred detectors as proposed in [4]. Both types of arrays improve considerably in threshold energy when located at high mountain altitude (see fig. 1).

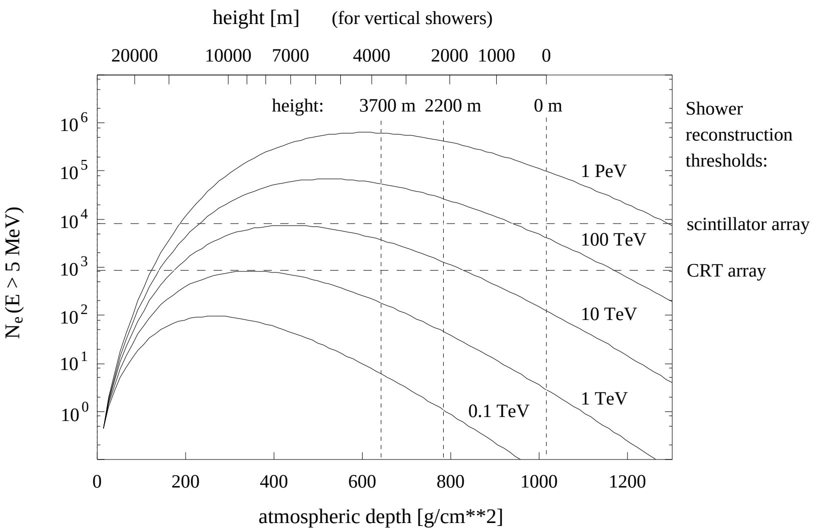

Figure 1: Illustration of the average longitudinal development of the number of $e^{\pm}$ with energy above 5 MeV in electromagnetic showers of various primary energies (0.1 TeV to 1 PeV). Approximate reconstruction thresholds for a typical scintillator array and the proposed CRT array are indicated. A CRT array at an altitude of 3700 m, for example, could achieve an energy threshold of about 3 TeV.

Apart from some detectors for locating the shower core, tracking detectors are not required to be spread out over a large area for reconstructing the shower direction. For scintillator arrays this is quite different because the arrival times of particles in the shower front jitter by tens of nanoseconds and a large lever arm is required for reconstructing the shower direction. Concentrating tracking detectors to a dense array can further reduce the energy threshold [10], without loss of accuracy although at the cost of a smaller array area and saturation of many detectors near the cores of large showers. The original CRT proposal called for an array of graded detector coverage with about 10% active area in the centre dropping to less than 0.2% near the periphery. Alternate layouts with a smaller number of CRT detectors in a dense array, surrounded by a halo of scintillators or other simple detectors for improved core location have also been considered.

The time projection chamber technique with large-volume drift chambers and proportional-wire readout via *flash analogue-to-digital converters* (FADC) was chosen for measuring the tracks of charged secondaries. This technique combines the advantages of a large-area detector, a fully three-dimensional track reconstruction, multi-hit capability, and few readout channels. Existing TPCs before CRT, however, were only operated in the tunnels of particle accelerators, at constant temperature and with continuous gas exchange. Operating tracking detectors in an experiment outdoor at mountain altitude is a quite different challenge. Temperatures may vary considerably from day to night. The detectors have to withstand rain, snow, and ice. Sudden power failures may occur. Operators might not be around all of the time and repairs might be difficult, if not impossible, on site. Therefore, CRT detectors had to be build as robust detectors and remote monitoring and control was an important requirement.

Another important aspect of the CRT design was to recognize muons in air showers. The primary γ-rays give rise to electromagnetic showers with very few muons while protons and nuclei initiate hadronic showers with more than an order of magnitude more muons. Therefore, the ratio of muons to other secondaries can be used to discriminate between the two types of showers. When searching for γ-ray sources, the isotropic hadronic background could be substantially reduced this way. CRT detectors use an iron plate between a top and a bottom tracking chamber as absorber for e^-, e^+, and γ secondaries. Most muons in air showers can easily pass through this absorber, with little scattering.

While a down-scaled, denser CRT array would have essentially the same energy threshold as the originally proposed array of 385 detectors, its sensitive area would be too small to effectively distinguish electromagnetic from hadronic showers already at threshold energies (about 3–5 TeV). Such a reduced array could be supplemented by other kinds of muon counters without tracking capabilities to achieve the initial goals.

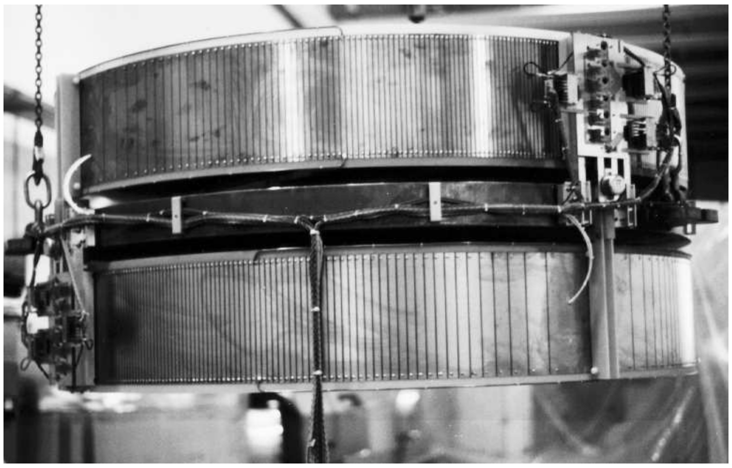

Figure 2: A CRT detector, with drift chambers and the iron plate, is ready to be moved into the container.

Figure 3: A CRT detector at the HEGRA site on La Palma with its electronics box opened.

3 The CRT detector module

3.1 Overview

A CRT detector consists of two large drift chambers of the TPC type [7] and a 10 cm thick iron plate in between (see fig. 2), all in a gas-tight container. To ensure pressure stability and to minimize the wall thickness of the container, a round cross-section of the apparatus was chosen. Initially, a spherical aluminium container was foreseen [4]. The modules described in this paper use a flatter stainless-steel container (see fig. 3) which promised improved gas quality due to clean surfaces and also improved robustness. The containers are produced by a standard manufacturing process for large steel vessels. Most of the electronics is

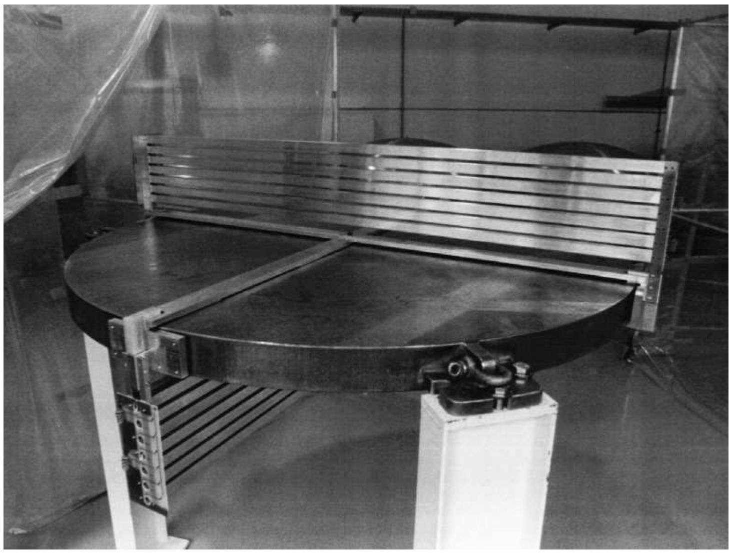

Figure 4: Wire chambers mounted with templates onto the iron plate. The templates are removed before the drift cages are mounted.

contained in a separate box. The size of the whole detector is chosen such as to fit into standard transport containers.

The original design [4] had a large scintillation counter underneath the upper drift chamber, just above the iron plate. Its main purposes were to provide a fast trigger and to allow an easy calibration of the drift velocity. To achieve a good gas quality, the scintillator had to be mounted in a gas-tight container on itself, making this counter difficult and expensive to produce. In the redesigned detector, the scintillator is not required. Instead, trigger electronics using the proportional wire signals was developed and upper and lower drift chambers are now mounted at right angles (fig. 4), enabling us to calibrate the drift velocity with penetrating muons (see Paper II). The detector is illustrated in figs. 2 and 5. The two circular drift chambers have a diameter of 1.8 m and a height of 26 cm, consisting of two D-shaped 'field cages' and a frame with six proportional wires in the middle.

In the drift chambers a homogeneous electrical drift field is sustained. Electrons from the tracks of ionizing particles drift along straight lines to a region near the sense wires. In the strong radial electrical field near the wires proportional gas amplification is used to obtain a detectable signal. The time t between the trigger and a signal provides the distance along the drift field between wire and track intersection (the x coordinate), except for an offset t_0 common to all signals from a track and for the drift velocity $v_{\rm d}$ as a calibration factor ($x = v_{\rm d}(t - t_0)$). In an air shower, most particles arrive within a few ten nanoseconds with respect to the 'shower front'. Thus, the same offset applies to all tracks from a shower in the same detector. The actual offset and the amount it may change from event to event depends on the trigger scheme (see sects. 4.6 and 4.7).

The y coordinate (along the wires) is obtained from charge-division readout of the wires and from signals induced on segmented cathodes. The third coordinate (z) is the height of the proportional wires themselves. The readout system was

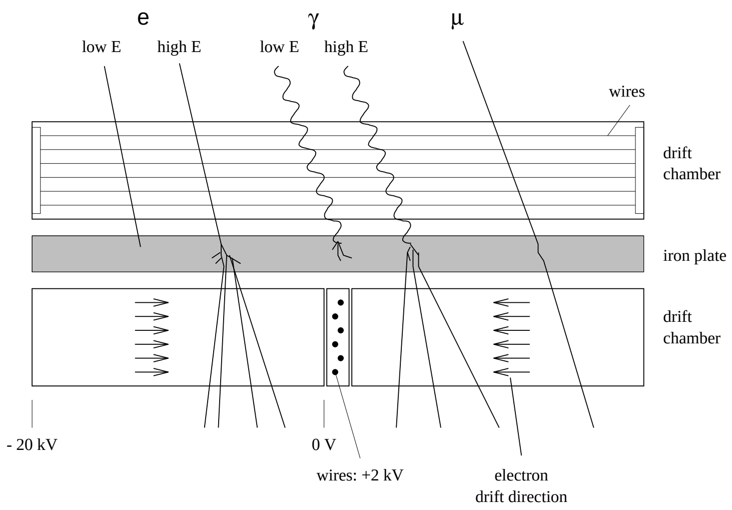

Figure 5: Schematical view of a CRT detector and the characteristics of various particle types.

designed to obtain the full 3-dimensional track information with a small number of readout channels.

The most frequent charged particle types can be very well distinguished by a CRT detector (see fig. 5). Electrons (e^+ and e^-) give rise to tracks in the upper chamber and are usually absorbed in the iron plate. High-energy electrons above a few hundred MeV – which are rare except very close to the showers axis – may cause electromagnetic showers in the iron plate with secondary electrons leaking through the iron plate. Similar showers might be caused by high-energy gammas, without corresponding tracks in the upper drift chamber. Such showers are usually recognized by having several tracks with almost the same intersection point in the iron plate and opening angles of tens of degrees. The muons easily penetrate the iron plate and are usually scattered by less than one degree. The only other particles with a good chance to be identified as muons are charged high-energetic hadrons. However, these are rare even in hadronic showers and can be found only close to the shower core.

3.2 Field cages

The field cages (fig. 2) have to maintain an uniform drift field. Their shape is defined by the geometry of the detector container and the iron plate. In order to have round drift chambers, the drift cages are D-shaped. Different field cage materials were tested, both in terms of performance and in terms of a possible large-scale production. The material of choice is 1.5 mm thick printed circuit board (PCB) made of glasfiber reinforced epoxy.

Potential lines are realized by 87 copper strips 7.62 mm wide and spaced by 2.54 mm on the plane upper and lower boards, parallel to the proportional wires. These boards are reinforced by two aluminium profiles. Upper and lower boards are connected by another board of 1 mm thickness bent around the circumference.

Here the strips start with the same 7.62 mm width near the wire chamber, getting wider and wider towards the opposite side in order to have the same projected strip period in drift direction (see fig. 2). The strips are both on the inner and outer sides of the PCBs, with outer strips overlapping gaps between inner strips and vice versa (see fig. 6) to minimize any field distortions from outside. All strips of the same potential are connected by bonds. Neighbouring strips on one of the plane boards are connected by resistors of $2.2\,\mathrm{M\Omega}$ ($\pm 1\%$), resulting in a voltage-divider resistance of $190\,\mathrm{M\Omega}$ per drift cage and $45\,\mathrm{M\Omega}$ in total for the $-20\,\mathrm{kV}$ power supply.

The ripple of the field due to discrete potential strips is smoothed out in the regions where drifting electrons may reach the proportional wires, since these regions are at least 24 mm, i.e. more than two strip periods, away from the upper and lower boards. In mounting the field cages, particular care was taken to make sure that the drift direction is perpendicular to the middle plane of the wire frame.

3.3 Wire chamber

The wire chamber in the middle plane of a drift chamber consists of the aluminium support structure, six sense wires, some of them with cathode boards mounted to the aluminium support (see figs. 4 and 6). The support structure consisting of seven aluminium profiles was chosen for several reasons. The aluminium profiles at ground voltage potential provide a very uniform termination of the drift field and decouple the proportional wire field from the drift field. By limiting the height of the track segment seen by a wire to 1 cm, the fall-off in resolution with increasing zenith angle due to ionization fluctuations along the particle tracks is effectively reduced. Furthermore, the aluminium structure holds the cathode boards and provides a robust support for the sense wires. The thickness of the material – 0.12 radiation lengths for vertical tracks passing through all seven profiles – is not a problem because only a very small fraction of all tracks in the detector cross the aluminium profiles.

The sense wires have a diameter of $28\,\mu\mathrm{m}$ and a resistance per unit length of $1740\,\Omega/\mathrm{m}$. They are mounted at alternate horizontal offsets (staggering) of ± 2 mm with respect to the middle plane of the aluminium profiles and are stretched by 0.7 N before they are fixed. Since the high-resistance stainless-steel wires cannot be soldered without chemically aggressive solvents, they are squeezed between the inside of a guard tube and a conical bolt.

Electron clouds from ionizing particles on both sides, i.e. in both drift cages, arrive at the wires and are amplified by a gas gain factor of about $4 \cdot 10^4$ in the radial field near the wires which are at a $+2000$ V potential, resulting in 10^6 electrons (0.16 pC) signals from minimum ionizing particles. At this gas gain and the expected rate of some 10^3 cosmics per second, the small space charge due to ions moving slowly through the drift field does not cause any significant field distortions.

Positions along the drift direction are determined from the drift time. For hits on a single wire it is impossible to tell from which side of the drift chamber the

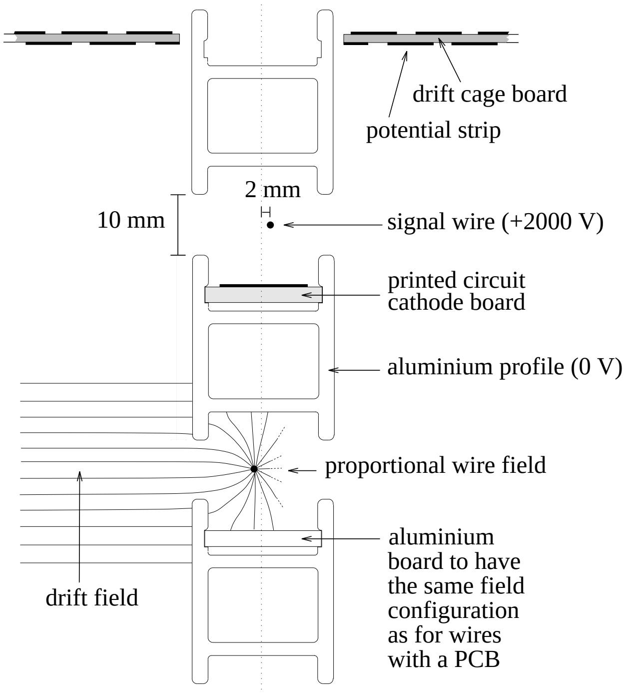

Figure 6: Cross section through part of the wire chamber showing the upper three of seven aluminium profiles and the upper drift cage boards on both sides.

electrons came. Due to the wire staggering this 'right-left' ambiguity is resolved when particle tracks are reconstructed (see Paper II).

For the reconstruction of positions along the wires some of the wires are equipped with a segmented cathode PCB. In the first four detectors only three cathode boards per chamber are used (on wires 1, 4, and 6, counted from the iron plate). Later detectors are built with four cathode boards per chamber (on wires 1, 3, 4, and 6). In principle, the charge induced on every cathode segment could be measured. To save electronics, every fourth of the 88 segments (*pads*) of 20.5 mm length, including a 0.5 mm gap, is connected to the same readout line. This causes a 22-fold ambiguity of the *pad coordinates*, i.e. the position along the wires reconstructed from the four cathode pad signals of a hit.

To resolve this ambiguity two of the wires with cathode boards (wires 1 and 4) are read out on both sides and positions along the wires are determined using the charge-division method. For this purpose a charge-division resolution of less than about one sixth of the 82 mm pad period length is required, i.e. about 0.75% of the wire length.

3.4 Container and muon filter plate

The purpose of the container vessel (see fig. 3) is to provide a hermetically sealed enclosure for the counting gas. The container also supports the muon filter plate (fig. 4), which in turn carries the drift chambers. With a large CRT array, detectors requiring a permanent flow of gas would be too expensive in terms of personal and money and too unreliable. The containers are made of 3 mm stainless steel and have an outer diameter of 216 cm and a height of 157 cm.

Two versions of the steel containers exist: one with a removable lid fixed by 32 screws to a 2.2 m diameter flange and a sealing ring in between, the other with a lid welded to the container. During detector development the containers with removable lid were used. After being sure that the detectors operated as intended, two of them were moved into the cheaper containers without flange and the containers were welded. A large detector array would use only welded-lid containers.

The muon filter is a 10 cm thick iron plate of 180 cm diameter and 2030 kg weight. The surface is passivated by galvanizing copper and nickel because any rust on it would spoil the gas quality, mainly with water vapour. Three screws fix the plate on supports welded to the vessel.

The containers have feed-throughs for high-voltage supplies, for twisted-pair cables for signals and monitoring, for preamplifier test-pulse cables, and for gas inlets and outlets. All feed-throughs are on a 55 cm diameter side flange and are protected against humidity and damage by a steel cover. This cover is connected to the external electronics box by a flexible tube to protect the cables.

3.5 Assembly and gas filling

All components obtained from manufacturers, like containers, iron plates, PCBs for drift cages and cathode pads, and aluminium profiles for the wire chambers were controlled to be within specifications. The wire chambers were assembled in a dedicated clean-room, all other major parts in a dust-poor environment. The drift cages were checked for proper connections of all strips on the same potential and for short-circuits with neighbour strips. To reduce surface contamination, all major components were cleaned with alcohol before the final detector assembly.

For the final assembly, the wire chambers were mounted to the iron plate using special templates to make sure that the two chambers were at right angles. The drift cages were mounted next, again with templates for proper positioning. Temperature, pressure, and orientation sensors were mounted to the wire chamber and the detector was cabled. All the cables were fixed to the iron plate to avoid accidental contact with the drift cages. The iron plate with drift chambers was placed into the container. The cabling was checked with test pulses, looking also for excessive noise or oscillations as evidence for grounding problems. Finally the container was closed, either by screws or by welding.

The detectors are operated in a 80-20 mixture of argon-methane. Because the containers would not withstand full evacuation, an efficient filling procedure was developed using an existing large-volume vacuum vessel. An entire CRT detector is moved into this vacuum vessel and both the vessel and the detector are evacuated for at least 12 hours. Most contaminations for the counting gas have then vanished. The detector is filled with argon-methane while the vacuum vessel is filled with air. This procedure is repeated after 2–3 weeks or before a detector is shipped. This way, an excellent quality of the counting gas is achieved with just two fillings.

The attenuation length, i.e. the length scale for attachment of drifting electrons to electronegative polluants, is a good measure for gas contamination. When it falls below about 1.5–2 m – typically some ten months after the first two fillings – the gas is exchanged. For a gas exchange on the experimental site a pump is attached to the detector container. The pressure in the container is reduced to about 400 mbar below the outside pressure and the detector is filled with new gas again. This pump-and-fill procedure is repeated four times with pure argon. Then methane is filled in and the gas mixture is good for at least another year, as the experience with the detectors on La Palma has shown.

3.6 Transport and installation

For the transport to the experimental site two detectors including electronics boxes and cables are loaded into a standard transport container.

At the experimental site the detectors are unloaded from the container with a crane and placed onto concrete foundations. After the cables from an electronics box to the corresponding detector and to the central station are connected, the power of the VME crate is turned on, and the online computer boots automatically. Then, the electronics is tested, the high voltages are turned on, and the detector is operational. The whole installation of two detectors is usually done by two persons on one day. None of the 10 detectors on La Palma suffered any damages on the transport.

4 The electronics and readout system

4.1 Overview

The detector stations are required to readout and process their data in parallel to and independent of each other, with a central trigger control and data collection. The readout and data acquisition system can be grouped into three major parts: the preamplifiers and monitoring devices inside the detector container, the electronics in the dedicated electronics box of each detector station, and the central station. The electronics box (fig. 7) is a weather-proof $60 \times 76 \times 35\,\mathrm{cm}^3$ metal box with a front-access door and forced-air cooling. It is located within about one meter from the side flange of the detector vessel.

Detector container and electronics box are connected by high-voltage cables, a test-pulse cable, and twisted-pair cables for signals and monitoring. The detector stations are connected to the central station for 220 V power supply, and by three RG 58 cables, one for computer communication via Ethernet, one for trigger signals from each detector station to the central trigger logic, and one for triggers plus event numbers sent from the central station to all detector stations (see fig. 8).

The electronics box contains the HV power supplies for the drift chambers (-20 kV) and the proportional wires ($+2.5$ kV, usually operated at 2.0 kV), pulse shaping units for the preamplified signals, FADCs, trigger electronics to generate local triggers from the wire signals of the detector and to process common triggers from the central station, monitoring electronics, and a local diskless computer

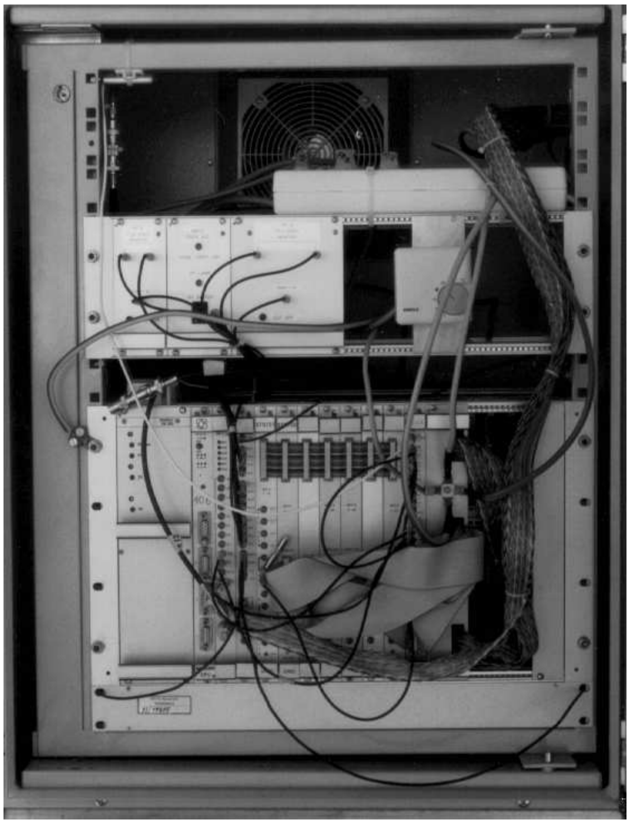

Figure 7: Open electronics box of a CRT detector. The VME crate with the CPU and readout electronics is in the lower, the high-voltage power supply in the upper part of the box.

system. Apart from the HV supplies, all units are in a single VME crate. Most of the electronics is custom-designed but is now available commercially.

The electronics in the central station of a CRT array consists of a VME system with the central trigger and event number logic and a workstation for collecting the data from the detector stations, further data processing, and backup. At the experimental site on La Palma island, interfaces to the HEGRA array exist for computer communication, trigger signals, event number distribution, and rubidium clock data including a 5 MHz counter. The main components of the whole setup and their interconnections are shown in fig. 8. In addition, networking devices and computer-controlled 220 V switches for the detector stations are important for the remote control of the whole CRT setup from Heidelberg.

4.2 Preamplifiers and shapers

Because about 3.5 m of cables are required from the wires and cathode pads to the electronics in the electronics box, preamplifiers inside the detector container are used to achieve an optimal signal-to-noise ratio. These preamplifiers work on both polarities and are implemented as charge-sensitive amplifiers in SMD technique, with eight small amplifier boards on a $8{\times}8$ cm^2 motherboard. One motherboard

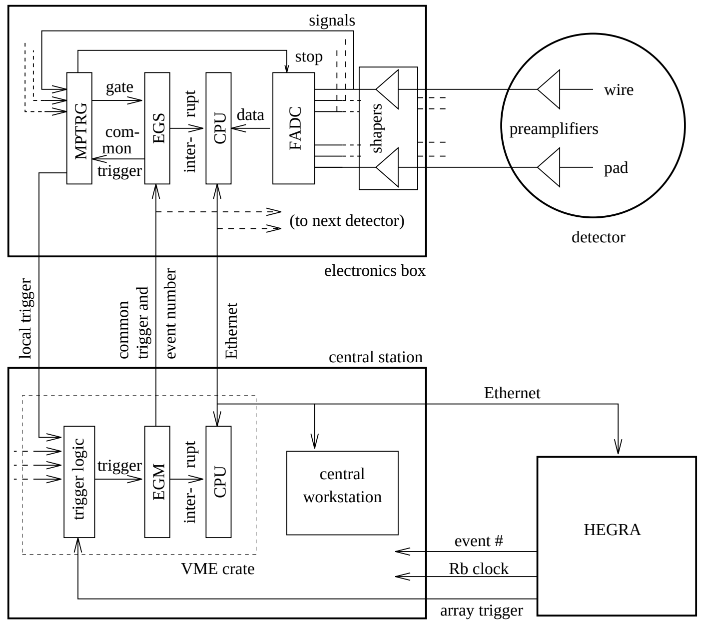

Figure 8: Schematical view of the main components of the readout and trigger electronics of the CRT array as set up on La Palma (*MPTRG*: trigger module, *EGM* and *EGS*: event number and trigger master and slave modules, respectively). For simplicity only one CRT detector is shown. Several detectors can be connected in series to the Ethernet and common trigger cables while for local (single detector) triggers each detector has a separate line to the central station.

for the wires and two for the cathode pads are needed per drift chamber. The amplification is three times larger for pad signals as compared to wire signals. Each motherboard is connected by a 20-wires twisted-pair cable to the gas-tight feed-throughs of the container and then to a set of eight corresponding shapers in the electronics box. The preamplifiers also have a test and calibration input which is connected to the fast DAC of the monitoring module.

The shaper circuits provide a differential receiver stage to reduce pickup on the cables, a dual pole-zero stage to compensate for the preamplifier pole and the $1/t$ tail of the proportional counter signals, and a low-pass to reduce spectral contributions beyond the Nyquist frequency of the 40 MHz FADC system. The preamplifier and shaper layout is shown in fig. 9. The identical system is used for both wire and pad signals, except that the shaper amplification is also a factor three larger for pads than for wires and that the pad signals are inverted in the shapers. Shaper units are implemented as a double-width VME module motherboard holding up to 48 SMD daughterboards with one shaper channel each and with connectors for six twisted-pair input cables and six flat output cables.

The dynamic range of the analogue electronics is limited by saturation of the preamplifiers and corresponds to more than 20 minimum ionizing particles at the usual gas gain around $4 \cdot 10^4$. In extremely busy events with many particles the amplifier will saturate. This is not considered as a serious problem because, even without saturation, the pattern recognition is difficult with more than 20 tracks.

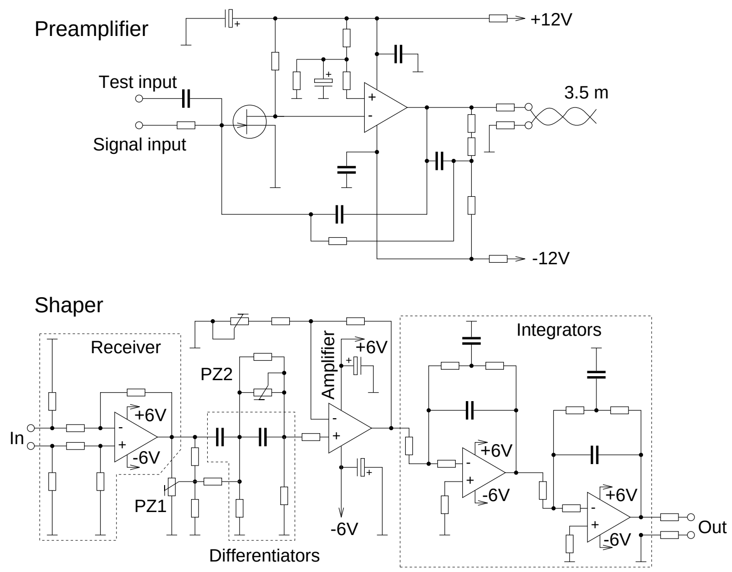

Figure 9: Schematical view of the preamplifier and shaper circuitry (PZ: pole zero).

The typical RMS noise is about 0.4 ADC counts for the wire signals and 2–3 counts for the pads.

4.3 Monitoring system

The monitoring system of a detector station consists of a VME module (*Monitor Module*, MPDTA 4/5/16) in the electronics box and several sensors in the detector container and the electronics box. In the detector container there are four temperature sensors, two inclination sensors, and one pressure sensor, connected via a 20-wires twisted-pair cable. In the electronics box are two temperature sensors and the 5 V and ±12 V voltages of the VME crate are monitored as well. The Monitor Module is also connected to the high-voltage power supply and to the test inputs of the preamplifiers.

The Monitor Module provides four TTL outputs, a 16-channel, 12-bit ADC multiplexed with 30 μs per channel, four slow (1 μs) 12-bit DACs, and one fast (10 ns) 12-bit DAC channel. The fast DAC is used to generate test inputs of the preamplifiers, two of the slow DACs set the +2.0 (max. 2.5) and −20 kV high-voltages. The ADC monitors the various sensors as well as the high voltage supply with monitoring outputs for both voltages and the corresponding currents. In case of current trips, the supplies can be reset via one of the TTL outputs.

The inclination sensors can be used to monitor any changes of the detector inclination in two perpendicular projections with a 0.01° resolution, although their absolute calibration is only accurate to a few tenths of a degree. The temperature and pressure sensors in the container are useful for remote checks of operating conditions and to indicate possible gas leakages. They could also be used to correct for changes in the drift velocity which is well correlated with the average temperature during the last few hours.

4.4 High voltage power supplies

High voltage power supplies suitable for the CRT detectors were obtained from two suppliers for the following specifications: 0 to +2.5 kV with up to 50 μA current and 0 to -20 kV with up to 600 μA current, long term stability better than 0.1%, ripple less than 0.01%, and temperature gradient less than 0.1%/K. For both output voltages the HV supplies have 0–10 V remote control inputs and 0–10 V remote monitoring outputs for voltages and currents but no manual control or display. If current limits are exceeded, the high voltage is switched off and the power supply has to be reset before voltages can be set up again. All control and monitoring of the HV power supplies is done by software via the Monitor Module.

4.5 FADC system

CRT detector stations have to record the amplitudes and timings of multiple signals on up to 48 channels. Both time and integral signal of the pulses are required for the track reconstruction. Traditional recording techniques with ADCs and TDCs are not suitable for CRT detector readout. Instead, the method of choice is to use *Flash ADCs* (FADCs) with parallel conversion and local memory for recording pulse shapes. Because existing FADCs were not compact enough, too expensive for a large CRT array, and consuming too much power due to ECL technology, a new VME-based FADC system (MPFA 40) was developed at the Max Planck Institute. An 8-bit converter chip in TTL technology is operated at a clock frequency of 40 MHz in the FADCs. In the development of the system great care was taken to eliminate glitches and spurious noise, and to provide a genuine 8-bit dynamic range.

The MPFA 40 system consists of two types of VME modules. The FADC modules (A40) have eight FADCs with 2 kbytes memory each, a VME interface for data readout, and a control bus interface to the controller module (C40). The C40 module transmits the *clock pulses* to synchronize up to 19 A40 modules in a VME crate, and the *data strobes* with an 11-bit address on the control bus. The same address is applied to the memories of all FADCs connected to the same controller. The FADCs are started (stopped) by enabling (disabling) the data strobes and the incrementing of the *Memory Address Register* in the controller. The controller allows a programmable delay between receiving a trigger signal and stopping of the FADCs.

For the CRT stations almost equal FADC pedestals (baselines) in all channels are desirable for easier and faster zero-suppression by software. For this purpose the pedestals of each FADC channel can be modified individually by corresponding DACs with a 0–0.9 V range. Common offsets of all channels of a FADC module can be changed with a potentiometer and a 10-bit DAC (0–1.8 V) on the controller module which can be connected to the *test inputs* of all FADC modules.

Due to the 2048-bytes memories the digitized signals from a time interval of up to 51.2 μs before the actual data-strobe stop are available for readout. The programmable delayed-stop feature is essential for CRT to select the time interval which should be read out after a stop signal (trigger). For different types of triggers, different delays are necessary. In the case of an internal trigger, the stop signal corresponds to the particle track closest to the proportional wires in an event. Other tracks further away from the wires may follow. The digitized signals from a short time before the trigger up to the maximum drift time after the trigger are required in this case. Therefore, the data strobe has to continue for at least another 14 μs after a trigger signal, assuming a drift velocity of about 65 mm/μs. The situation is similar for a prompt external trigger from a scintillator array. In the case of a trigger from an array of CRT detectors, however, the stop signal is delayed at the central station and no delay of the FADC stop is required.

4.6 Local trigger

To derive a local trigger from the drift chamber signals and to combine it with the common trigger from the central station, a special VME module (*Trigger Module*, MPTRG 11/8) was developed for CRT. This module has a fully programmable 2-kbytes lookup table with 20 ns access time for eleven logic inputs (addressing bits) and eight logic outputs (data bits). Due to the lookup table, eight independent outputs can be programmed for 2048 independent input conditions. The first eight inputs (A0–A7) have discriminators with programmable thresholds and gate generators with programmable widths, the other three (A8–A10) are TTL inputs. The first output bit is connected to two TTL outputs (D0 and D0c) with independently programmable widths, the others are connected to one TTL output each. Three outputs (D1–D3) have widths as defined by the width of the trigger-overlap (80 ns minimum), the other four outputs (D4–D7) are latched and have to be reset by software. A 32-bit counter can be used to monitor the trigger rate on any of the eight outputs to evaluate the local system deadtime.

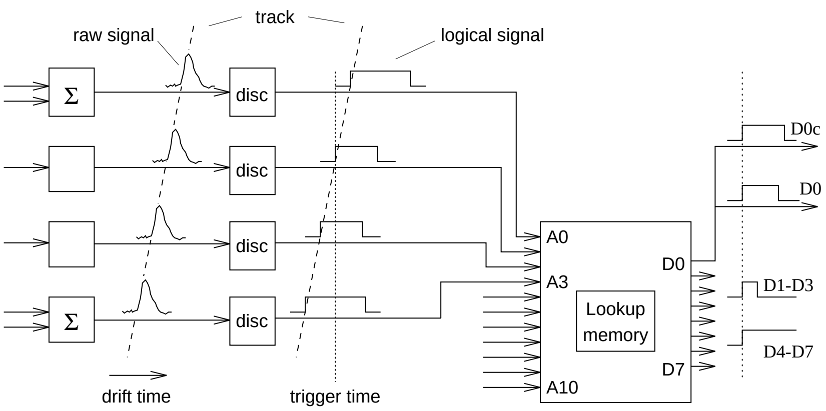

Figure 10: Part of the local trigger logic (for 3-out-of-4-wires trigger of upper drift chamber). The track corresponding to the raw and logical signals is superposed. Analogue signals from both ends of a charge-division wire are summed up (Σ) before the discriminator and gate generator stage ('disc').

By means of piggy-back boards different configurations of signals can be routed to the first eight inputs. For CRT the signals of the four wires next to the iron plate from each chamber are used (see fig. 10). The two analogue signals per charge-division wire are summed up on the piggy-back board. To avoid any trigger bias, the electronics gains of both channels should, therefore, be roughly the same. The piggy-back board is connected to the flat cables from the shapers to the FADCs.

The trigger of a CRT detector is fully under software control. Typical trigger conditions for operating stand-alone detectors are 3 out of 4 wires in the upper chamber, 3 out of 4 in any chamber, or in both chambers depending whether mainly electrons, any type of particle, or mainly muons are wanted. The A0–A7 discriminators have a *hysteresis* or threshold of 40 mV, corresponding to about 10% of the average signal amplitude of minimum ionizing particles. Effective trigger thresholds are of the same order. The hysteresis rules out random triggers due to noise on the wire signals. A high trigger efficiency for charged particles penetrating the drift chamber is achieved. For a single-wire efficiency of $\epsilon_1 = 95\%$, the total efficiency of a 3-out-of-4 trigger is about 98.6% while a 4-out-of-4 trigger would have a total efficiency of only 81%.

Because trigger conditions for each output channel are independent, the trigger module can be used to stop the FADC by a coincidence of wire signals or by an external trigger from the central station and, at the same time, to provide a local trigger to the central station and gate signals to other VME modules in the same electronics box. The trigger module provides no CPU interrupt. This remains the task of the FADC master module or the Event Grader Slave module described in the following section.

4.7 Central trigger and event number distribution

The detector-station computers run independent of each other and without any strict synchronization mechanism which would cause large and unpredictable dead-times for a large array of CRT detectors. Therefore, each central trigger has to have an unique identifier (*event number*) which can be used to link the data from different detectors for the same event later.

The solution developed for CRT is a system of transmitters and receivers for central trigger signals and the associated event numbers. The transmitter in the central station (*Event Grader Master*, MPEGM or EGM) is supplied with the lower 16 bits of the next event number to be used and enabled for the next trigger. When receiving a trigger the EGM sends a trigger pulse after a small and fixed delay and immediately appends the 16-bit event number as 16 pulse-length encoded bits plus two parity bits and additional control bits. By this method, event numbers corresponding to an array trigger are available at all stations at the time of FADC readout without additional overhead for synchronizing the detectors.

The Event Grader Master can be connected directly to several receivers (*Event Grader Slaves*, MPEGS or EGS) at detector stations in series or via one or more dedicated repeaters (*Event Grader Repeaters*, MPEGR or EGR). Repeaters can be connected by optical fibers over large distances or by coaxial cables over up to a few hundred meters.

Instead of transmitting trigger signals and event numbers the EGM can also transmit control codes, either to all detectors in common or to individual detectors, by using different values of the control bits. Control codes to individual detectors consist of a 12-bit station number and 4 bits available both as TTL outputs on the EGS control panel and via a VME register. Of the 16-bit numbers received simultaneously by all slave modules, 12 bits are used to extend the event number and 4 others are also available as TTL outputs. Furthermore, the EGM/EGS system allows to measure the propagation delay from the central to any detector station and back to better than 1 ns.

The EGS can be programmed to interrupt the CPU when any selected type of signal is received or a parity error occurs. Triggers are accepted in coincidence with a local gate signal provided by the trigger module. This way, the gate can be either opened all the time or only for a fixed time interval after a local trigger at the detector station, depending on the programming of the trigger module. In a large CRT array only a small fraction of the detectors would be hit by particles of a typical shower. Therefore, the local interrupt rate at a detector station can be reduced by about an order of magnitude if gate intervals are used.

The EGM can similarly interrupt the CPU of the central VME system computer after receiving a signal from the central trigger logic, in order to set the next 16-bit event number, to read out other modules, and to enable the EGM again. Among the modules read out in the central station on La Palma are a 16-bit input register module (*VME Digital Input/Output*, VDIO) and an interface for a Rubidium clock (*Clock Interface*, MPCLKI). The VDIO is used to receive an event number from the HEGRA data acquisition system. The Clock Interface module was developed for receiving the time and date information as well as 1 Hz and 5 MHz counts from a Rubidium clock and latching them after a common trigger. VDIO and MPCLKI readings are used to provide cross reference information between the independent event numbers of CRT and HEGRA when combining the data offline.

5 Final remarks

In the Cosmic Ray Tracking project, a detector system with tracking detectors of the TPC type and muon identification has been developed. Ten of these detectors are in operation on La Palma for up to two years now, without any major failures. Experience with these ten detectors has shown that the CRT detectors are robust enough for long-term operation at mountain-altitude conditions. The online software, including data reconstruction and detector calibration procedures, is described in Paper II. The detector performance has been found to meet or even exceed the initial goals (see also Paper II).

Acknowledgments

We would like to thank the members of the HEGRA collaboration for their help during buildup and operation of the CRT detectors on La Palma. The Gesellschaft für Schwerionenforschung (GSI), Darmstadt, designed the steel detector containers and provided the equipment to galvanize the iron plates. The CRT project was partially supported by the Bundesministerium für Forschung und Technologie.

References

[1] J. Wdowczyk, J. Phys. G20 (1994) 1001.

[2] J. W. Cronin, K. G. Gibbs, and T. C. Weekes, Ann. Rev. Nucl. Part. Sci. 43 (1993) 883.

[3] J. Heintze et al., Cosmic Ray Tracking – ein neuer Weg für die γ-Astronomie bei hohen Energien, Proposal an das BMFT, 1988.

[4] J. Heintze et al., Nucl. Instr. and Meth. A277 (1989) 29.

[5] M. Feuerstack et al., Addendum to the proposal 'Cosmic Ray Tracking – a new approach to high-energy γ-astronomy', 1990.

[6] S. Polenz, PhD thesis, Heidelberg, 1994.

[7] T. Lohse and W. Witzeling, in Instrumentation in high energy physics, ed. F. Sauli, pp. 81–155, World Scientific, Singapore, 1992.

[8] K. Bernlöhr et al., Online software and performance of the Cosmic Ray Tracking detector system, submitted Nucl. Instr. and Meth. A, 1995 (Paper II).

[9] F. Aharonian et al., in Proc. of 23rd Intern. Cosmic Ray Conf., Vol. 4, p. 291, University of Calgary, 1993.

[10] K. Bernlöhr, Space Sci. Rev. (in press), 1995.